Supplementary information

Multifunctional nanoscale lanthanide metal-organic framework based ratiometric fluorescence paper microchip for visual dopamine assay

Long Yu [1], Lixiang Feng [1], Li Xiong, Shuo Li, Qi Xu, Xiangyu Pan and Yuxiu Xiao*

Key Laboratory of Combinatorial Biosynthesis and Drug Discovery (Ministry of Education), and Wuhan University School of Pharmaceutical Sciences, Wuhan 430071, China

[1]These authors contributed equally to this work

*Corresponding author at: Wuhan University School of Pharmaceutical Sciences, Wuhan 430071, China.

Tel.: +86 27 68759892; fax: +86 27 68759850.

E-mail address: yuxiuxiao2011@whu.edu.cn, 99783508@qq.com (Yuxiu Xiao).

Contents:

Partial experimental section

Reagents and chemicals

Europium (III) nitrate hexahydrate ($Eu(NO_3)_3.6H_2O$) was purchased from Saan Chemical Technology Co., Ltd. (Shanghai, China). Dopamine (DA) and N, N-dimethylformamide (DMF) were obtained from Aladdin Bio-Chem Technology Co., LTd. (Shanghai, China). Resorcinol was supplied from Adamas Reagent Co., Ltd. (Shanghai, China). 1,3,5-Benzenetricarboxylic acid (H_3BTC) was purchased from Macklin Biochemical Co., Ltd. (Shanghai, China). L-Glycine and tris(hydroxymethyl)methyl aminomethane THAM (Tris) were obtained from Lingfei Technology Co., Ltd. (Jiangsu, China). Copper (II) chloride dihydrate ($CuCl_2 \cdot 2H_2O$) was supplied from Sinopharm Chemical Reagent Co., Ltd. (Shanghai, China). DA solution and resorcinol solution were prepared using water as solvent.

Instrumentation and characterization

The fluorescence excitation and emission spectrum were measured by the FL-4600 fluorescence spectrophotometer (Hitachi, Japan). UV-2600 UV-vis spectrophotometer (Shimadzu Co., Ltd., Japan) was devoted to survey the absorption spectrum. In addition, series of the apparatus were applied for characterization of materials. The Zeiss Ultra Plus thermal field emission scanning electron microscope (SEM) (Carl Zeiss AG, Germany) was used to observe the morphology of the MOF. The Fourier transform infrared spectroscopy (FT-IR) of MOF powder was characterized by Thermo-Nicolet NEXUS 470 infrared spectrometer (Thermo Fisher Scientific, USA). The powder X-

ray diffraction pattern (PXRD) that related to crystal structure was performed on Bruker D8 Advance diffractometer with Cu Kα radiation (Bruker AXS, Germany). In order to realize the qualitative analysis and quantitative analysis of copper element, the measurement was carried on the Thermo Scientific K-Alpha X-ray photoelectron spectrometer (Thermo Fisher Scientific, USA) and ContrAA700 Atomic Absorption spectrometer (Germany), respectively. As for the azamonardine product, the ^{1}H and ^{13}C spectra were recorded on AVANCE III NMR spectrometer (400 MHZ, Bruker AXS, Switzerland) and the deuterated reagent is d_6-DMSO. The ultrahigh resolution mass spectrometer (Thermo Fisher Technology Co., Ltd., Q EXACTIVE, China) was used to get the precise molecular weight. Other conventional instrument, SevenEasy S20 desktop pH meter (Mettler-Toledo Instruments Co., Ltd., China); ME-55 Analytical Balance (Mettler-Toledo Instrument Equipment Co., Ltd., China); H1850 High-speed Centrifuge (Xiangyi Instrument Co., Ltd., China); MX-S vortex mixer (Dalong Xingchuang Experimental Instrument Co., Ltd., China); Milli-Q ultrapure water system (Millipore, France).

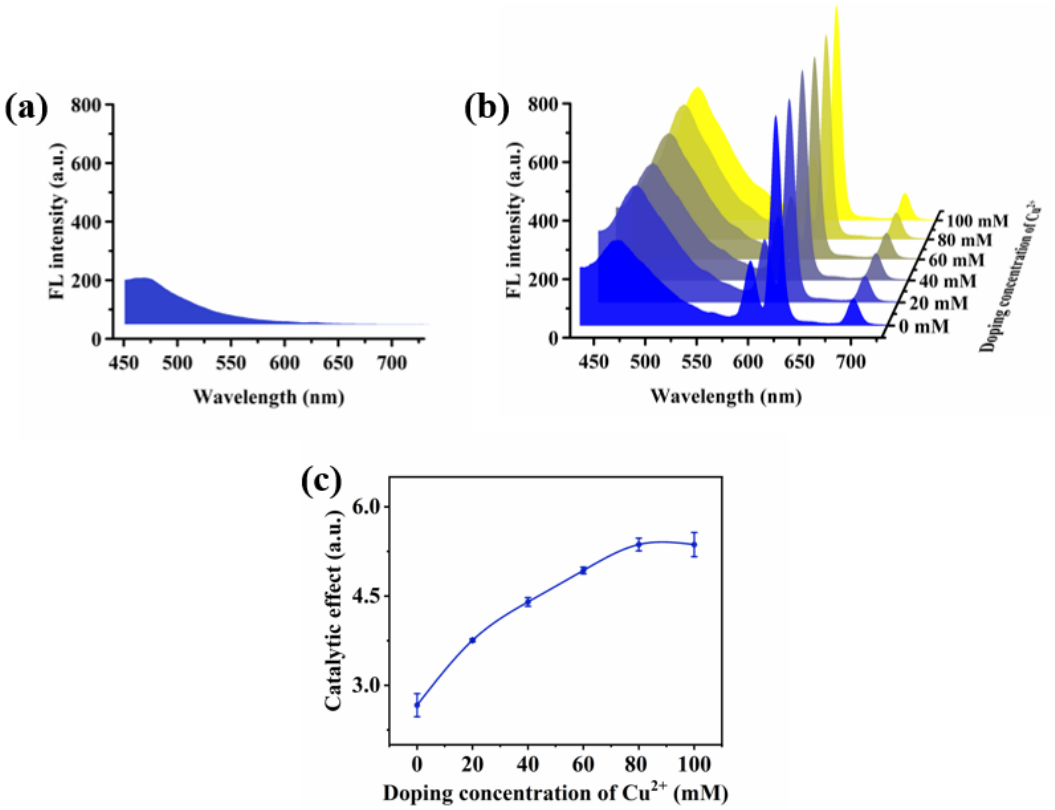

Fig. S1 The optimization of the doping concentration of Cu^{2+}. (a) Control group: 20 μM dopamine and 20 μM resorcinol, reacting for 20 min in 10 mM tris-glycine buffer (pH 9.0); (b) experimental group: 20 μM dopamine and 20 μM resorcinol, 100 μg mL^{-1} Cu@Eu-BTC, reacting in 10 mM tris-glycine buffer (pH 9.0) for 20 min. Catalytic effect: $I_{464\ nm\ (experimental\ group)}/I_{464\ nm\ (control\ group)}$.

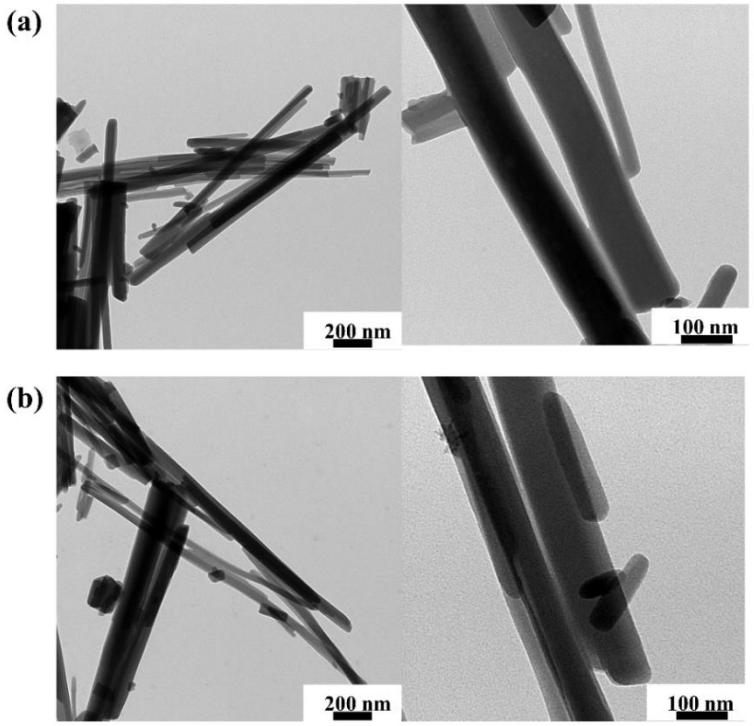

Fig. S2 (a)The TEM image of Eu-BTC; (b) the TEM image of Cu@Eu-BTC.

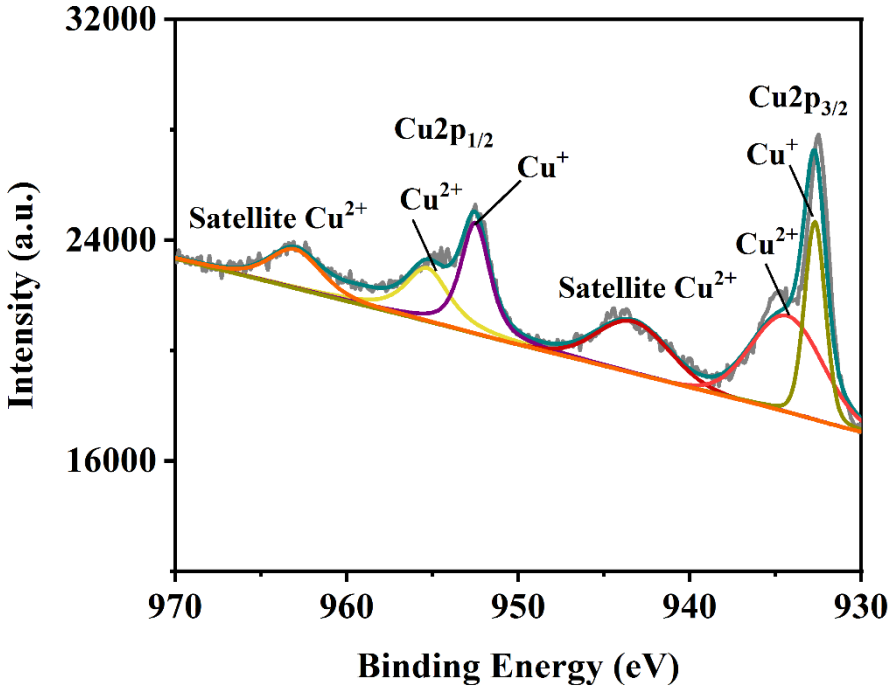

Fig. S3 The XPS fine spectra of Cu@Eu-BTC (Cu 2p). The results show that not only Cu^{2+} is observed, Cu^{+} is also observed, which is due to the defects in the MOF and the incomplete surface framework structure.[1]

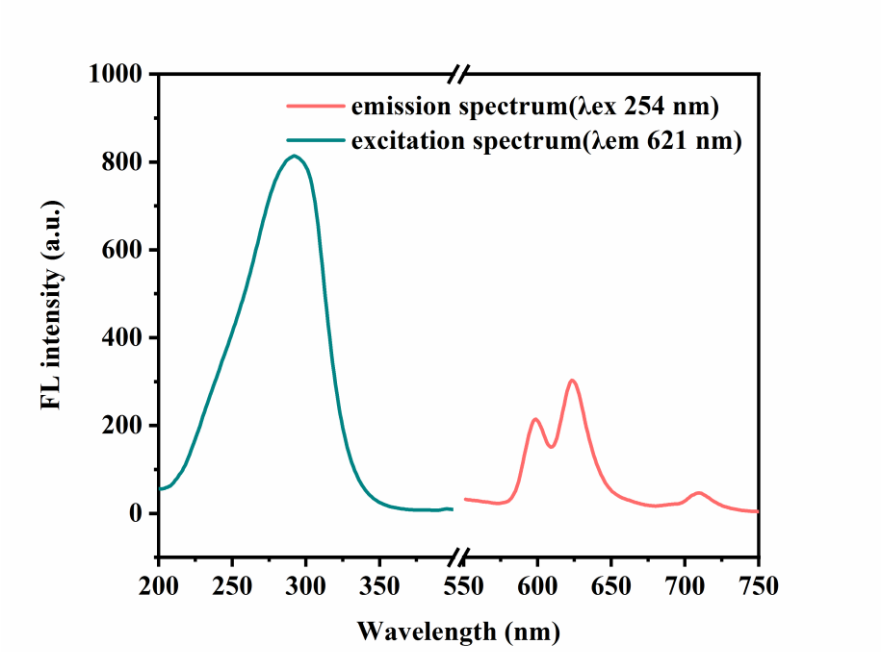

Fig. S4 The excitation and emission spectra of 50 μg mL^{-1} Eu-BTC dispersion in tris-glycine buffer (pH 9.5, 20 mM).

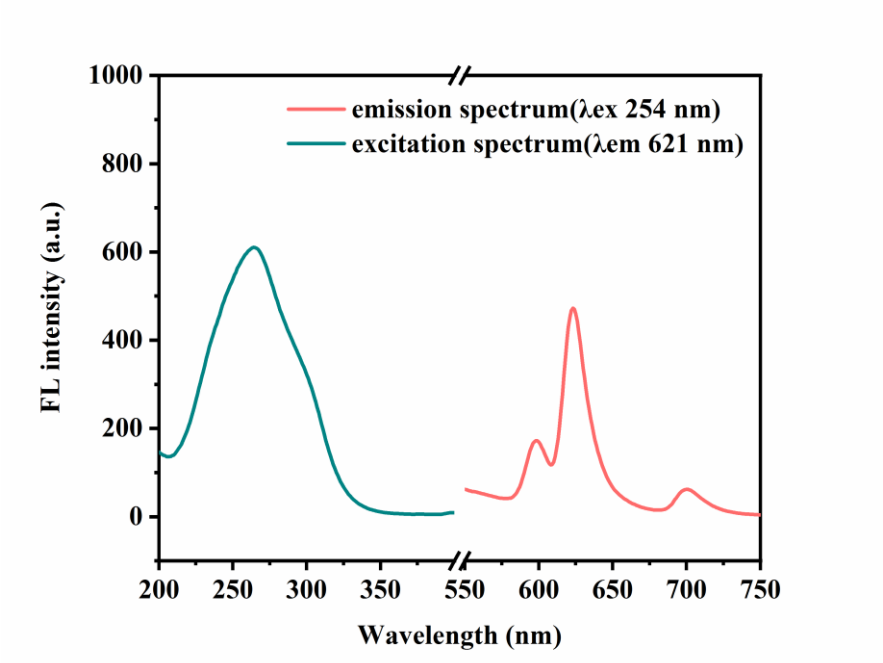

Fig. S5 The excitation and emission spectra of 50 μg mL^{-1} Cu@Eu-BTC dispersion in tris-glycine buffer (pH 9.5, 20 mM).

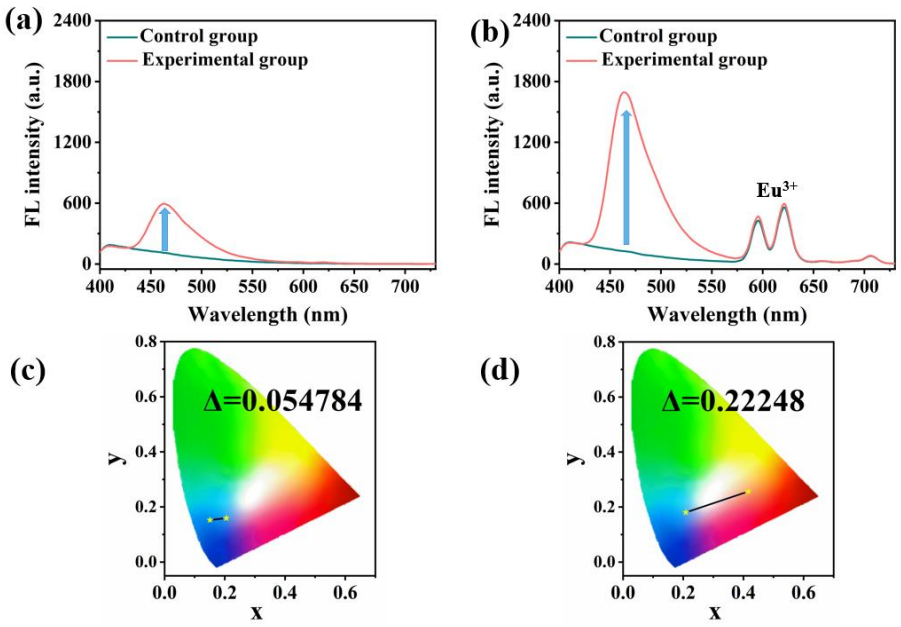

Fig. S6 (a) the fluorescence spectra without Cu@Eu-BTC for DA assay; (b) the fluorescence spectra with Cu@Eu-BTC for DA assay; (c) the CIE image transformed from (a); (d) the CIE image transformed from (b). Control group: the detection system containing no DA; Experimental group: the detection system containing 20 μM DA. Other conditions for the detection system: 20 mM tris-glycine buffer, pH 9.5, resorcinol concentration 150 μM, and reaction time 20 min.

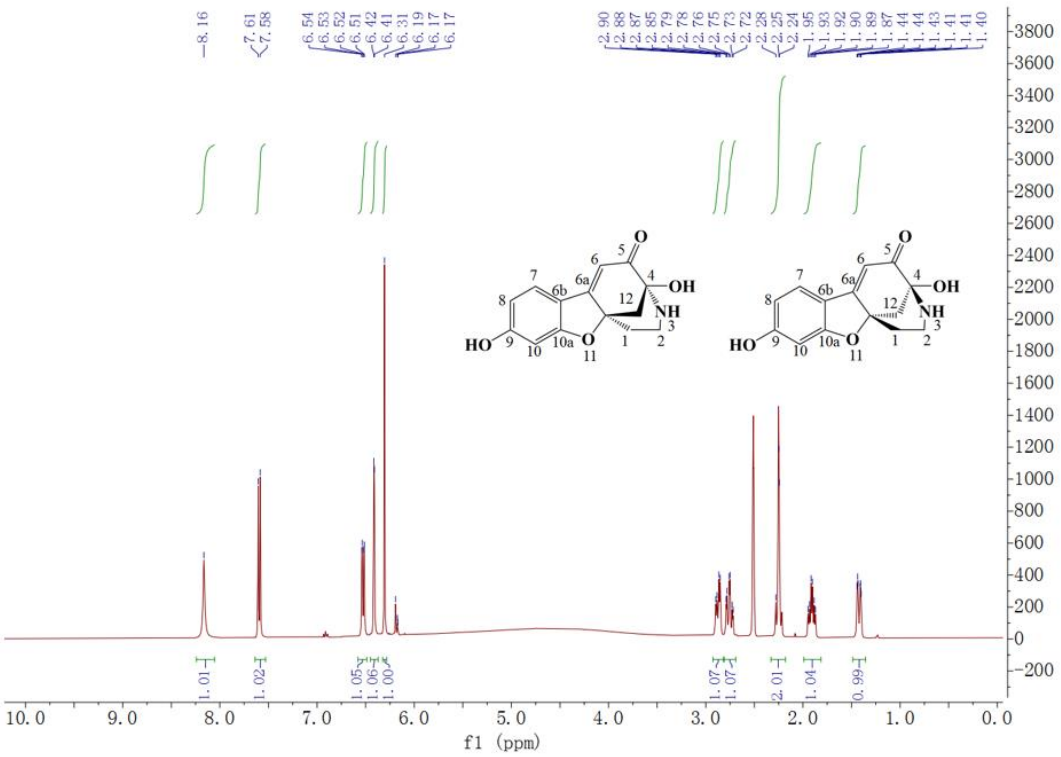

Fig. S7 The ^{1}H-NMR spectrum of reaction product azamonardine.

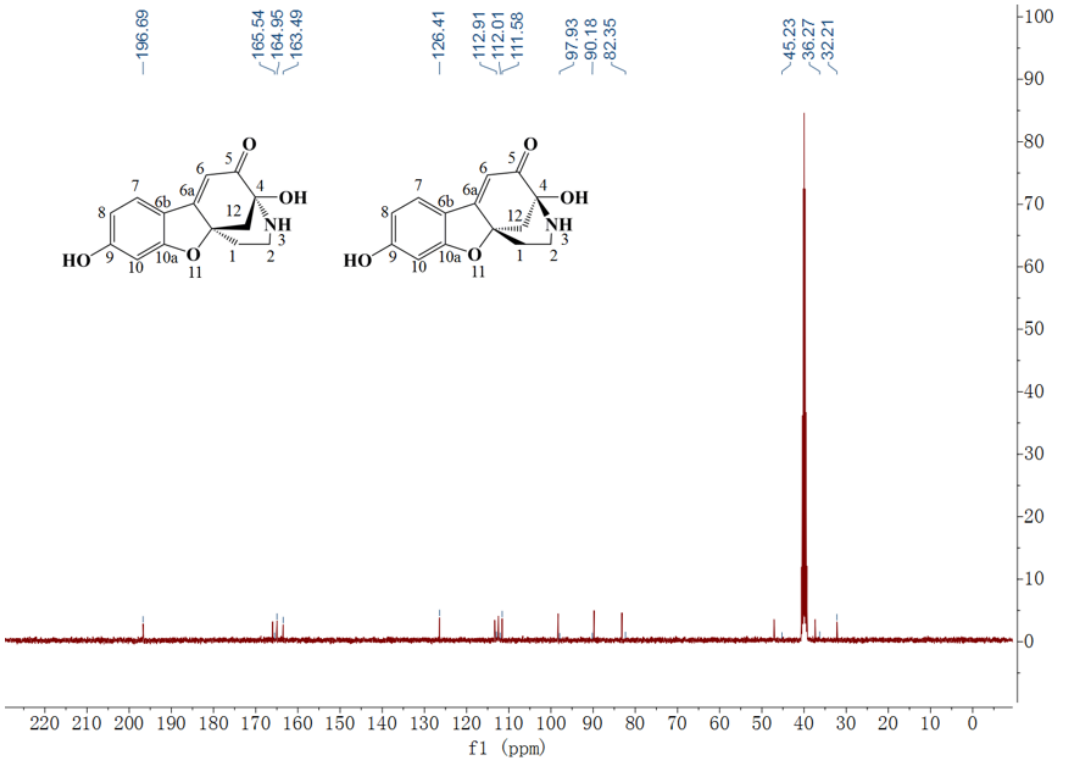

Fig. S8 The ^{13}C-NMR spectrum of reaction product azamonardine.

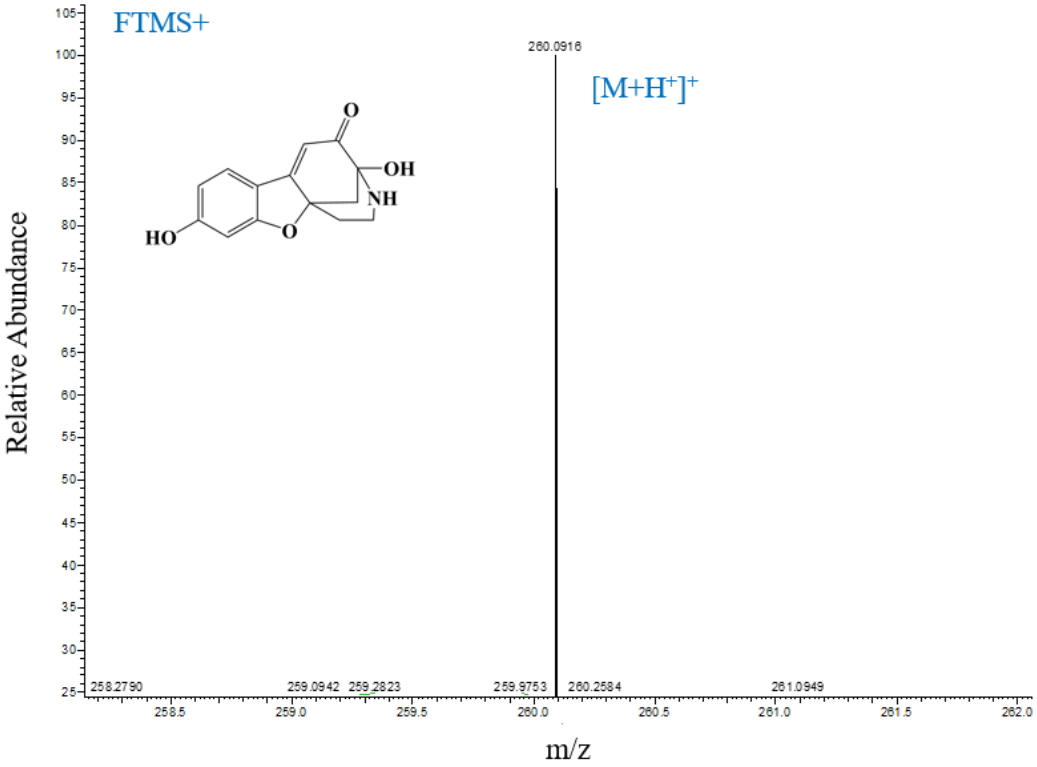

Fig. S9 The high-resolution mass spectrometry result of reaction product azamonardine.

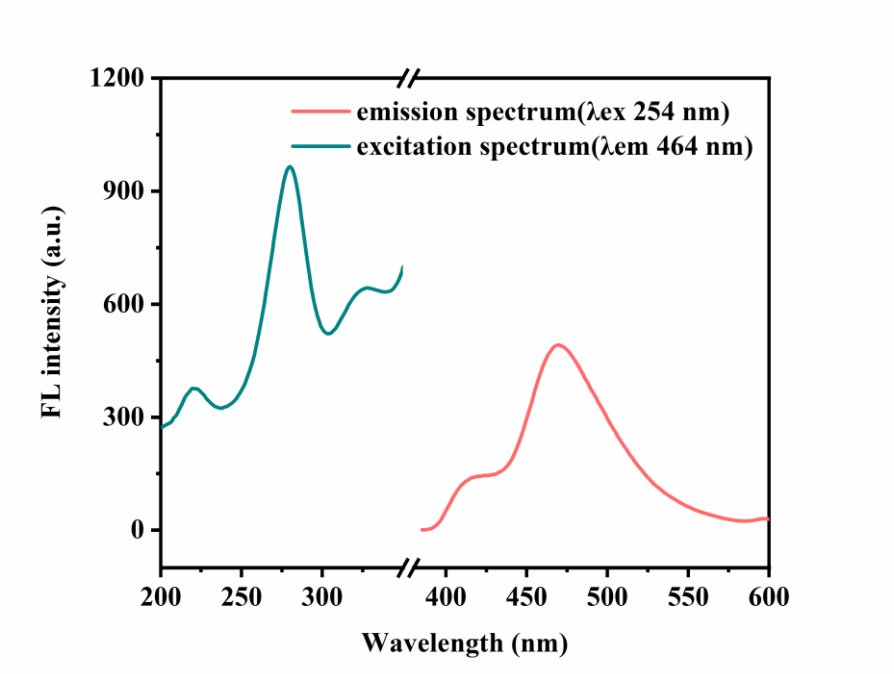

Fig. S10 The excitation and emission spectra of 2 μM azamonardine solution in tris-glycine buffer (pH 9.5, 20 mM).

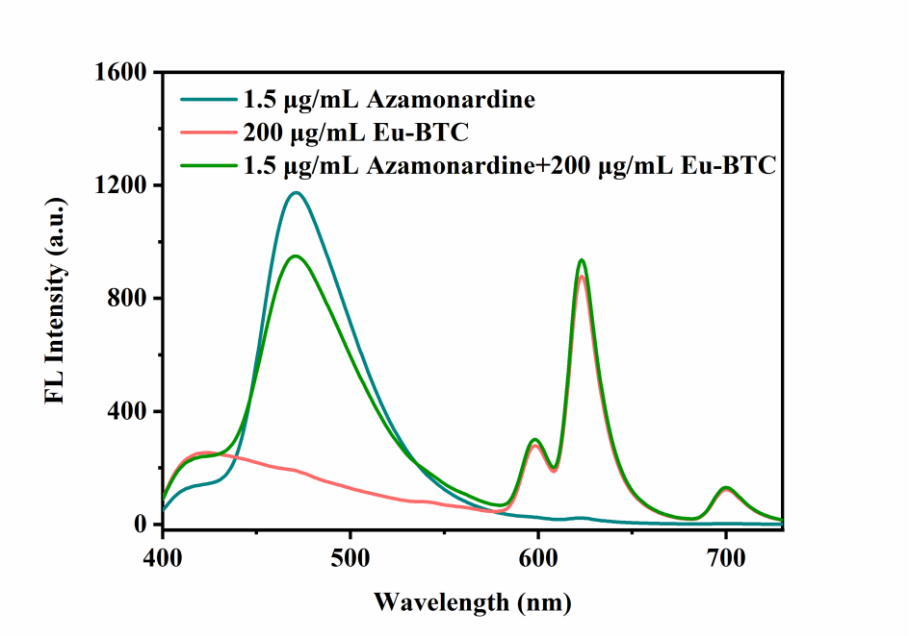

Fig. S11 The fluorescence spectra for verification of AIE effect of Eu-BTC in tris-glycine buffer (pH 9.5, 20 mM).

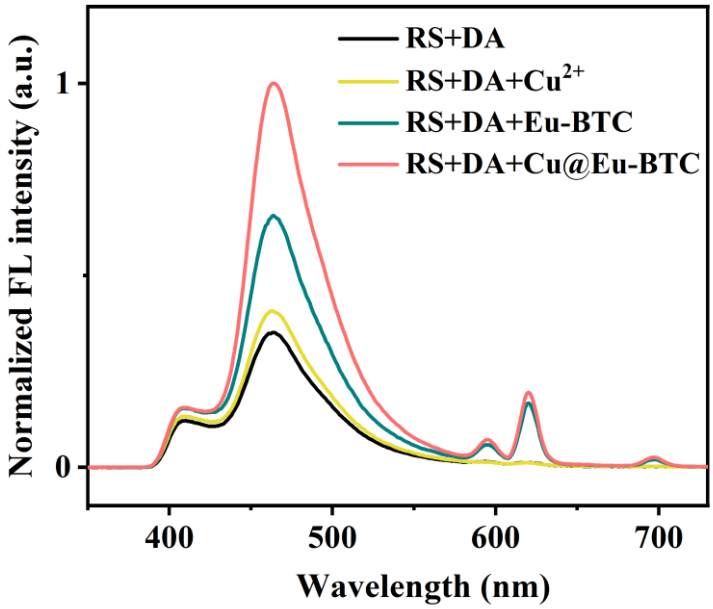

Fig. S12 The fluorescence spectra of reaction between RS and DA with Cu^{2+}, Eu-BTC, Cu@Eu-BTC or without any substance. The concentration of Cu^{2+} is 2.79 μM (which is equivalent to the Cu^{2+} content in 50 μg mL^{-1} Cu@Eu-BTC), the concentration of Eu-BTC and Cu@Eu-BTC is 50 μg mL^{-1}. 20 mM tris-glycine buffer, pH 9.5, resorcinol concentration 150 μM, DA 20 μM, and reaction time 20 min.

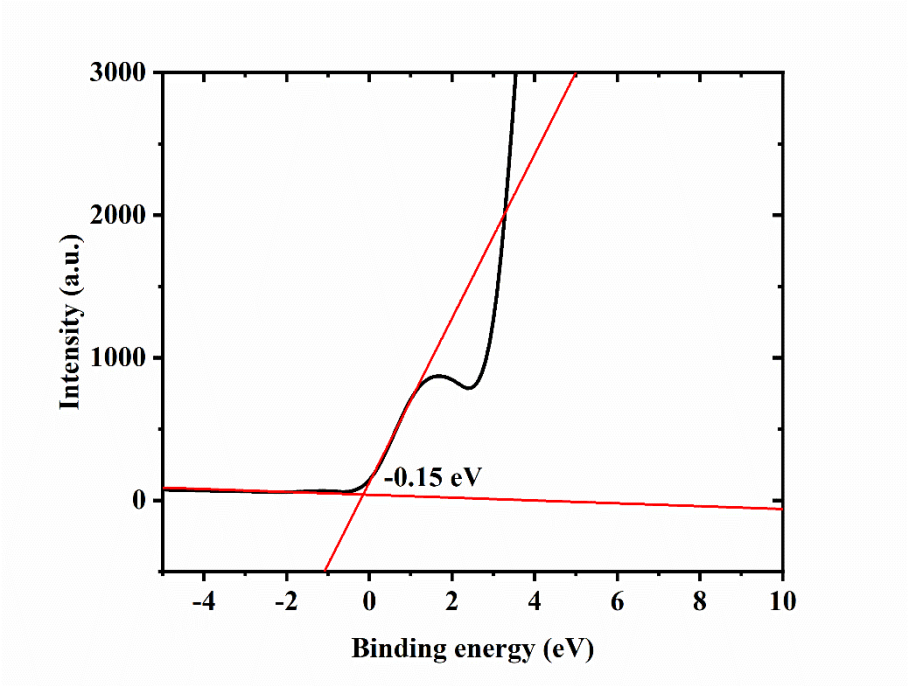

Fig. S13 The valence-band XPS spectrum of Eu-BTC.

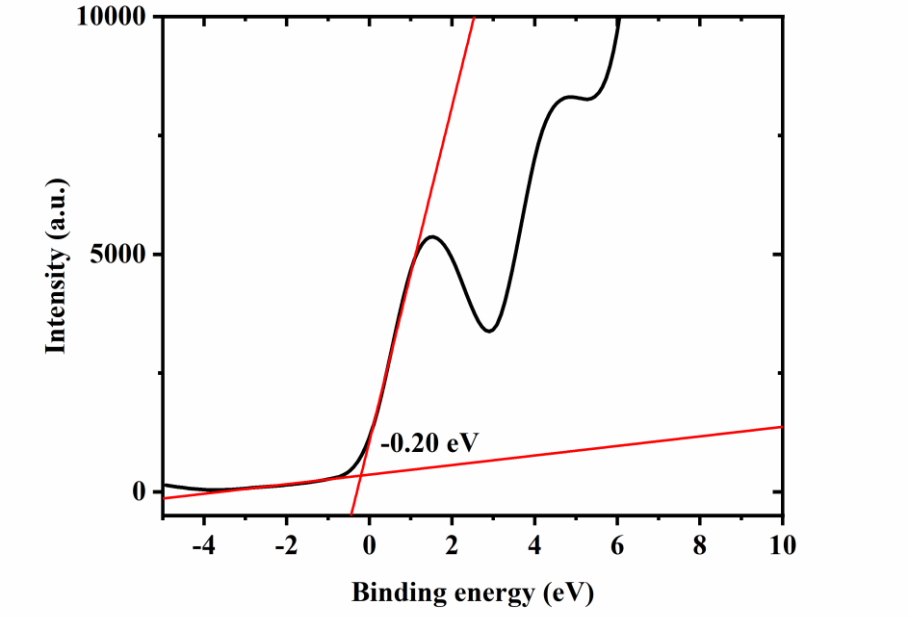

Fig. S14 The valence-band XPS spectrum of Cu@Eu-BTC.

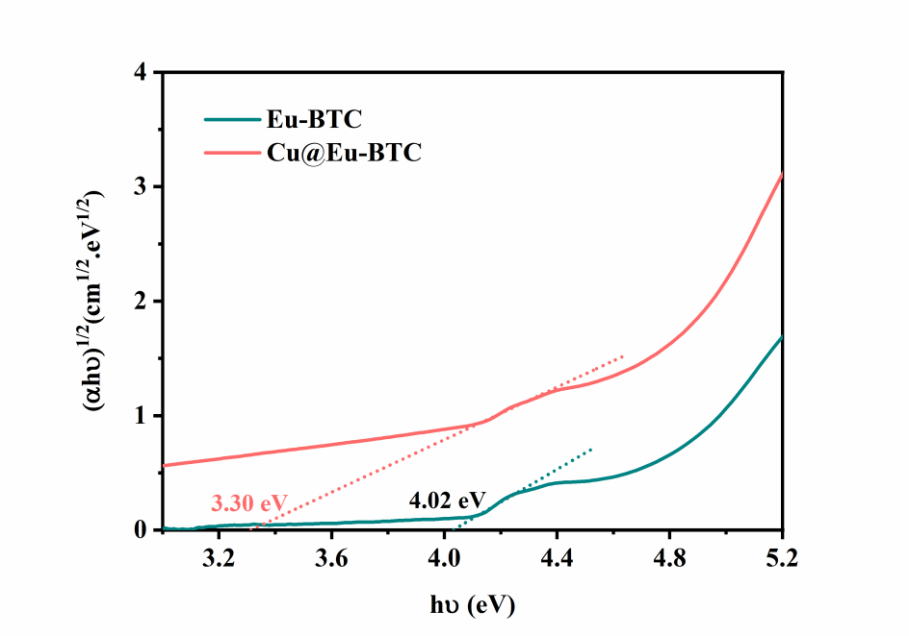

Fig. S15 The $(\alpha h\nu)^{1/2}$ versus hν curve of Eu-BTC and Cu@Eu-BTC. The band structure is calculated by the KubelKa-Munk (KM) method according to the equation: $\alpha h\nu = A(h\nu - Eg)^2$, where α is the absorption coefficient, h is Planck's constant, ν is frequency, Eg is the direct band gap, and A is a constant.

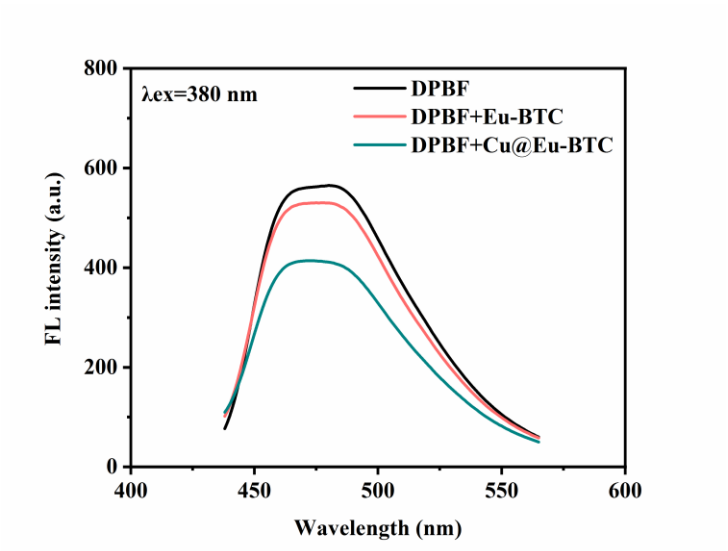

Fig. S16 The $^1O_2$ capture experiment. Diphenylbenzofuran (DPBF) is used as a $^1O_2$ capture agent at a concentration of 200 nM, the concentration of Eu-BTC and Cu@Eu-BTC is 200 μg mL^{-1}, reaction time is 1 h, and the excitation wavelength is 380 nm. (The results indicate that Cu@Eu-BTC can produce more $^1O_2$ compared to Eu-BTC because the fluorescence of DPBF is quenched after DPBF captures $^1O_2$.)

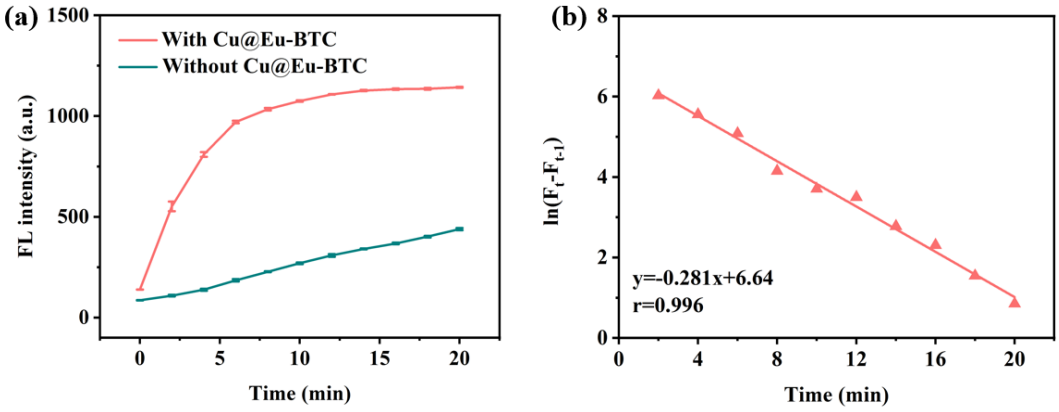

Fig. S17 (a) The kinetic experiment for the evaluation of the catalytic activity of Cu@Eu-BTC (comparison of the difference between the presence and absence of Cu@Eu-BTC); (b) the determination of the catalytic rate constant of Cu@Eu-BTC, F stands for fluorescence intensity, t stands for time. The concentration of Cu@Eu-BTC is 50 μg mL^{-1}. 20 mM tris-glycine buffer, pH 9.5, resorcinol concentration 150 μM, DA 10 μM, and reaction time 20 min.

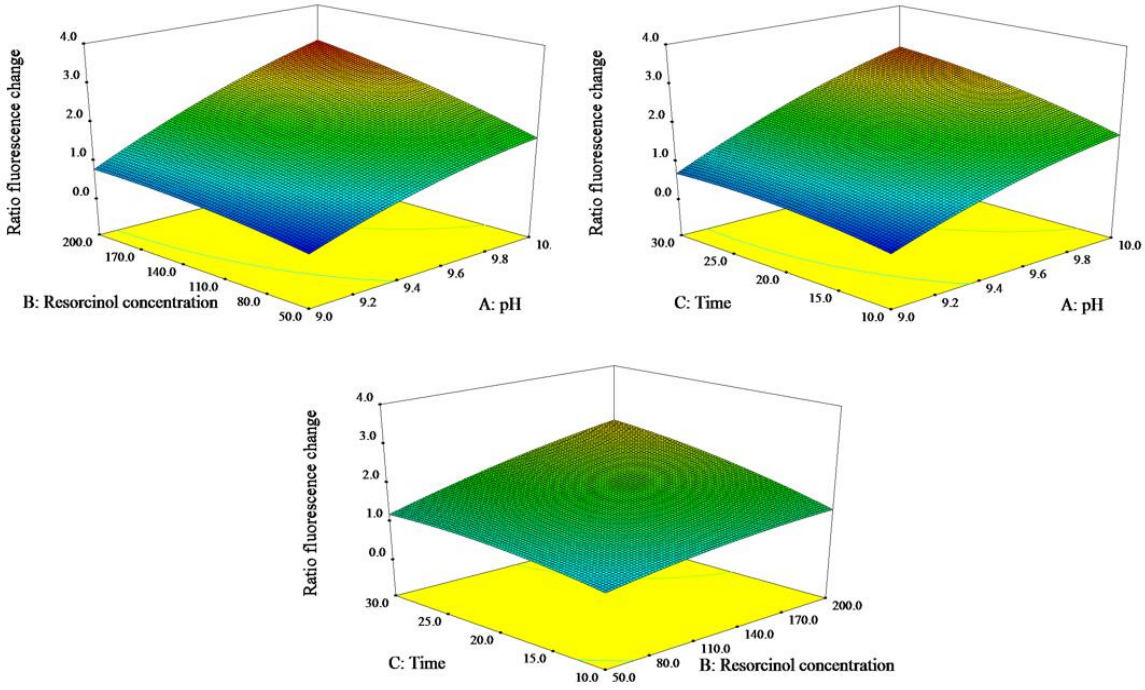

Fig. S18 Response surface curves about the influence of reaction pH (A), resorcinol concentration (B, μM) and reaction time (C, min) on the ratio fluorescence change for dopamine assay.

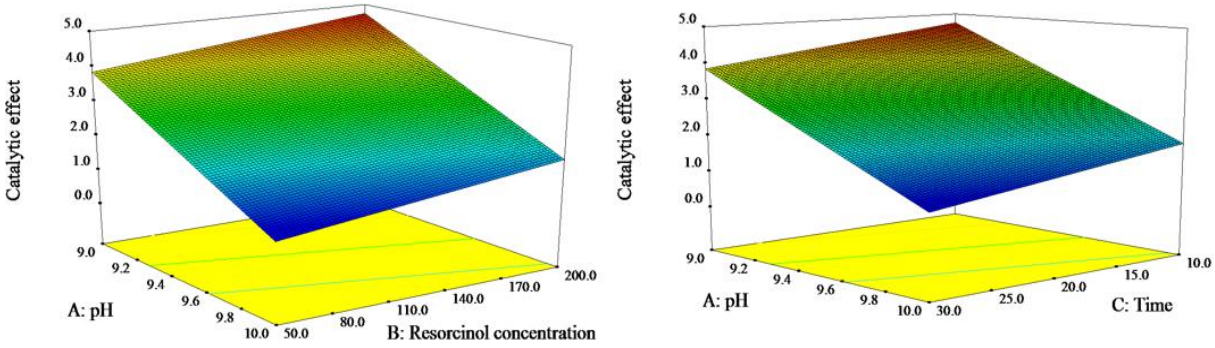

Fig. S19 Response surface curves about the influence of reaction pH (A), resorcinol concentration (B, μM) and reaction time (C, min) on the catalytic effect for dopamine assay.

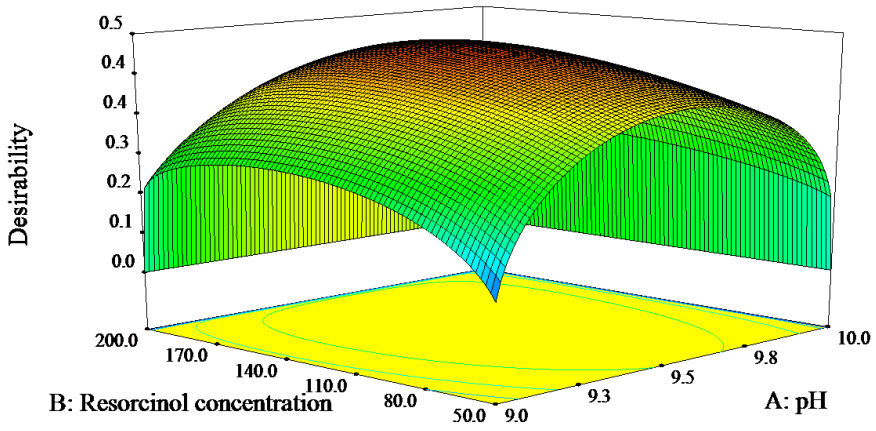

Fig. S20 Response surface curves about the influence of reaction pH (A), resorcinol concentration (B, μM) on the combination of ratio fluorescence change and catalytic effect for dopamine assay.

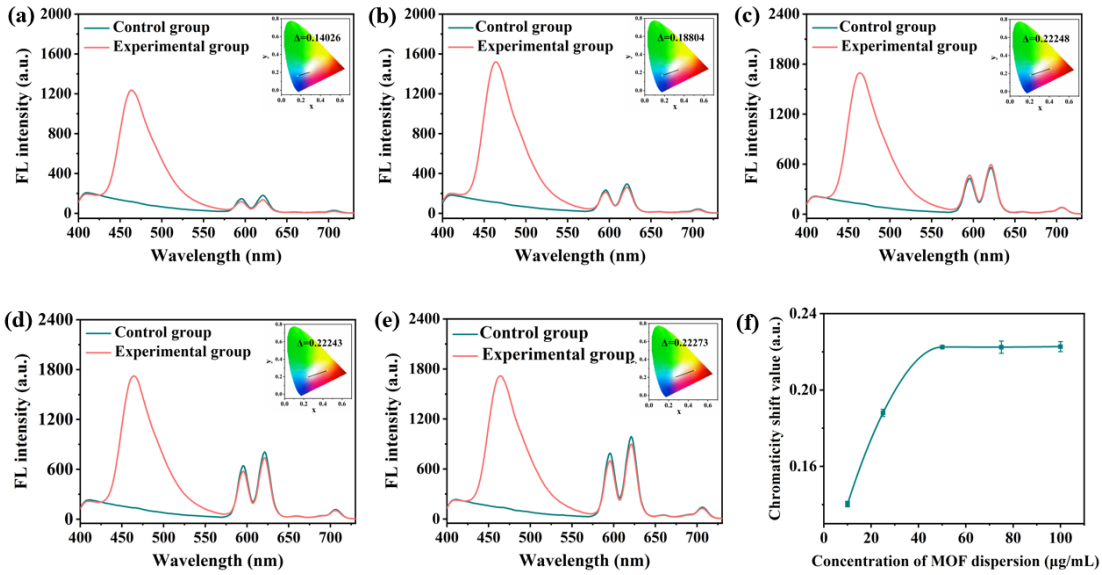

Fig. S21 The optimization of Cu@Eu-BTC concentration for DA detection. The fluorescence spectrum of the detection system with Cu@Eu-BTC concentration of 10 μg mL^{-1} (a), 25 μg mL^{-1} (b), 50 μg mL^{-1} (c), 75 μg mL^{-1} (d), and 100 μg mL^{-1} (e), respectively; (f) the varying trend of chromaticity shift value with the MOF concentration. Control group: the detection system containing no DA; Experimental group: the detection system containing 20 μM DA. Other conditions for the detection system: 20 mM tris-glycine buffer, pH 9.5, resorcinol concentration 150 μM, and reaction time 20 min.

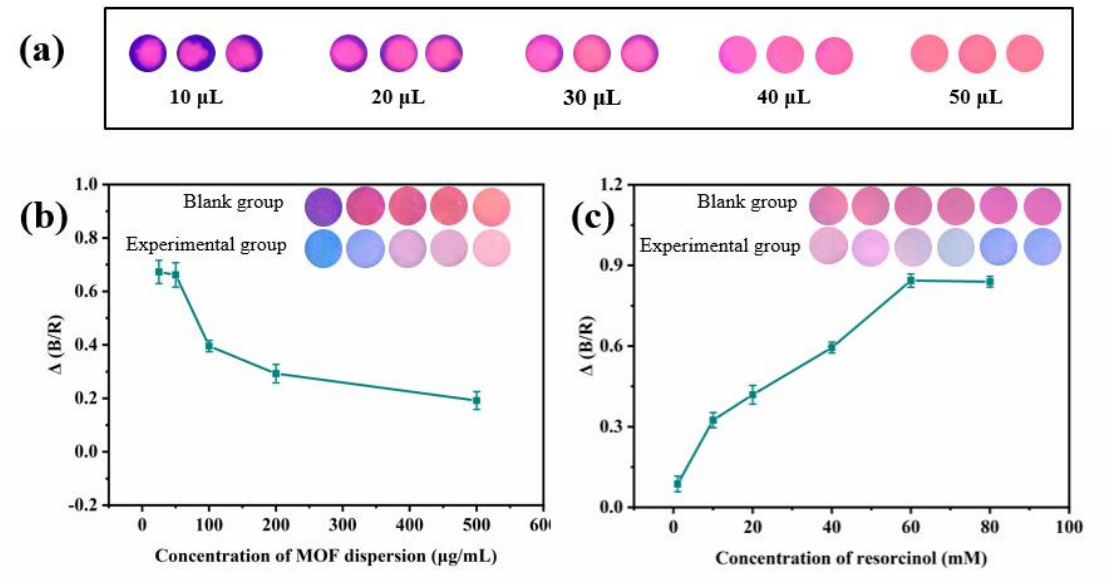

Fig. S22 (a) Volume optimization of Cu@Eu-BTC MOF dispersion added to paper base (MOF dispersion :100 μg/mL). (b) The concentration optimization of Cu@Eu-BTC dispersion (pH value: 9.5; tris-glycine buffer: 20 mM; DA concentration: 10 μM; reaction time: 10 min; resorcinol concentration: 60 mM; MOF dispersion volume: 40 μL). (c) The concentration optimization of resorcinol solution (pH value: 9.5; tris-glycine buffer: 20 mM; DA concentration: 10 μM; reaction time: 10 min; MOF dispersion: 50 μg/mL and 40 μL).

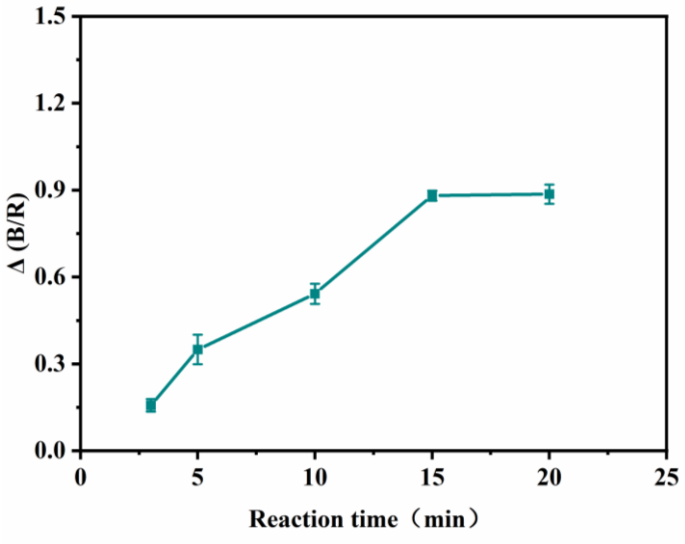

Fig. S23 The reaction time optimization for visual DA assay. (pH value: 9.5; tris-glycine buffer: 20 mM; DA concentration: 10 μM; resorcinol concentration: 60 mM; MOF dispersion: 50 μg/mL and 40 μL)

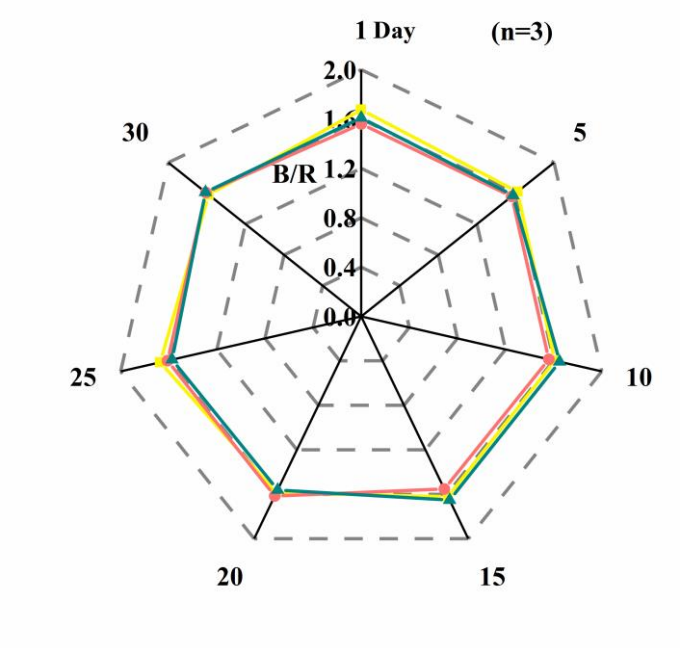

Fig. S24 The storage stability of DA paper biosensor in 30 days (n = 3). The stability of MOF-loaded paper was investigated by serum samples diluted with 20 mM tris-glycine buffer (pH=9.5) every four/five days within a month（DA: 10 μM; reaction time: 15 min; resorcinol concentration: 60 mM).

Table S1 Experimental results for Box-Behnken design: three factors are reaction pH, resorcinol (RS) concentration and reaction time

Run	Factor			Response	
	pH	RS concentration (μM)	Time (min)	Ratio fluorescence change	Catalytic effect
1	9.5	125	20	1.8593	3.0191
2	9	50	20	0.3336	4.4035
3	10	125	30	2.8395	1.4233
4	9.5	50	10	0.8929	2.5749
5	9.5	125	20	1.6369	2.5862
6	9.5	200	30	2.5071	2.7078
7	9.5	125	20	1.6816	2.6385
8	9.5	125	20	1.8199	2.7462
9	10	125	10	1.7183	1.3984
10	10	50	20	1.7246	1.1925
11	9	200	20	0.7428	4.419
12	9.5	200	10	1.4106	4.3241
13	9.5	50	30	1.1964	1.7082
14	10	200	20	3.0697	1.9574
15	9	125	30	0.7463	3.7514
16	9	125	10	0.4197	4.8137
17	9.5	125	20	1.8020	3.0188

Table S2 ANOVA and validation of response surface model for the optimization of dopamine assay conditions (response index 1: ratiometric fluorescence change)

Source	Sum of square	Degree of freedom	Mean square	*F*-value	*p*-value
Model	9.78	9	1.09	149.90	<0.0001**
A-pH	6.32	1	6.32	871.23	<0.0001**
B-RS concentration	1.60	1	1.60	221.22	<0.0001**
C-Time	1.01	1	1.01	139.78	<0.0001**
AB	0.22	1	0.22	30.20	0.0009**
AC	0.16	1	0.16	21.76	0.0023**
BC	0.16	1	0.16	21.68	0.0023**
A^2	0.14	1	0.14	19.13	0.0033**
B^2	0.052	1	0.052	7.12	0.0321*
C^2	0.092	1	0.092	12.62	0.0093**
Lack of Fit	0.014	3	7.25E-003	0.52	0.6904
Residual	0.051	7	4.75E-003		
Pure Error	0.036	4	9.12E-003		
Cor Total	9.83	16			
R^2	0.9948				
Adjusted R^2	0.9882				
Predicted R^2	0.9710				
Experimental value (n=3)	1.91±0.071				
Error in relation to Predicted value (%)	-2.05				

* Significant, $p < 0.05$. ** Highly significant, $p < 0.01$. RS: resorcinol.

The model equation:

Ratiometric fluorescence change =

1.76+0.89 * A+0.45 * B+0.36* C+0.23 * A * B+0.20 * A * C+0.20*B * C-0.18 * A^2- 0.11* B^2- 0.15* C^2

The adjusted coefficient R^2 is 0.9882, which proves the reliability and accuracy of the model. The predicted R^2 is 0.9710, which is in reasonable agreement with the adjusted coefficient R^2, indicating that the model can effectively predict the experimental results. The *p*-value of the model is less than 0.0001, which proves that the regression model is significant. In addition, factors A, B and C all have a significant impact on the ratiometric fluorescence change, and there is an interaction between AB, AC, and BC ($p < 0.05$). In addition, the *p*-value of lack of fit is 0.6904 ($p > 0.05$), indicating that the fitting result of the model is highly credible.

Table S3 ANOVA and validation of response surface model for the optimization of dopamine assay conditions (response index 2: catalytic effect of Cu@Eu-BTC)

Source	Sum of square	Degree of freedom	Mean square	*F*-value	*p*-value
Model	19.40	3	6.47	53.02	<0.0001**
A-pH	16.29	1	16.29	133.58	<0.0001**
B-RS concentration	1.56	1	1.56	12.77	0.0034**
C-Time	1.55	1	1.55	12.70	0.0035**
Lack of Fit	1.41	13	0.16	3.69	0.1108
Residual	1.59	9	0.12		
Pure Error	0.17	4	0.043		
Cor Total	20.98	16			
R^2	0.9244				
Adjusted R^2	0.9070				
Predicted R^2	0.8506				
Experimental value(n=3)	3.00±0.18				
Error in relation to Predicted value (%)	2.68				

* Significant, $p < 0.05$. ** Highly significant, $p < 0.01$. RS: resorcinol.

The model equation:

$$\text{Catalytic effect} = 2.86 - 1.43 * A + 0.44 * B - 0.44 * C$$

The adjusted coefficient R^2 is 0.9070, which proves the reliability and accuracy of the model. The predicted R^2 is 0.8506, which is in reasonable agreement with the adjusted coefficient R^2, indicating that the model can effectively predict the experimental results. The *p*-value of the model is less than 0.0001, which proves that the regression model is significant. In addition, factors A, B and C all have a significant impact on the catalytic effect of Cu@Eu-BTC. In addition, the *p*-value of lack of fit is 0.1108 ($p > 0.05$), indicating that the fitting result of the model is highly credible.

Table S4 Charge distribution analysis of resorcinol, DA, epinephrine and norepinephrine

Species	Resorcinol		DA		Epinephrine		Norepinephrine	
	D	A	D_1	A_1	D_2	A_2	D_3	A_3
Charge distribution	-0.712	0.063	-0.529	0.159	0.018	0.334	-0.358	-0.258

Table S5 Ratiometric chromaticity (B/R) in the nine different circular areas (3*3) of three paper microchips obtained after being Immersed in the aqueous dispersion of Cu@Eu-BTC (100 μg mL^{-1}) with different volume

Area	10 μL		20 μL		30 μL		40 μL		50 μL	
	B/R	SD	B/R	SD	B/R	SD	B/R	SD	B/R	SD
1	1.925		0.808		0.828		0.741		0.534	
2	0.839		0.892		0.917		0.741		0.586	
3	0.892		0.808		0.808		0.776		0.534	
4	1.000		0.851		0.808		0.776		0.567	
5	1.138	0.512	1.375	0.194	0.802	0.061	0.733	0.018	0.552	0.021
6	0.862		0.862		0.776		0.741		0.586	
7	1.248		0.741		0.857		0.733		0.534	
8	2.305		0.808		0.741		0.765		0.580	
9	1.145		1.048		0.925		0.733		0.567	

SD: standard deviation

Table S6 Comparison of the proposed method in this work with other fluorescent methods for the assay of DA in human serum

Methods	Catalytic fluorescence turn-on reaction	Visual assay	Ratiometric chromaticity	Paper microchip	LOD (μM)	Linear range (μM)	Ratiometric fluorescence	Reference
UiO-66-NH_2	no	no	no	no	0.68	1-70	yes	2
Eu-DBA	no	no	no	no	0.015	0.05-30	yes	3
Carbon quantum dot	no	no	no	no	0.158	0.25-50	no	4
$NaGdF_4$: Tb	no	no	no	no	0.033	0-20	no	5
Eu-ECP	no	no	no	no	0.021	0.1-10	no	6
C-dot	no	no	no	no	0.125	0-100	no	7
Carbon nanodot	no	no	no	no	0.22	1-10	no	8
Cu@Eu-BTC	yes	yes	yes	yes	0.01	0.04-30	yes	this work

UiO-66-NH_2, University of Oslo-66-NH_2; **Eu-DBA**, Eu-3,5-dicarboxybenzeneboronic acid; **Eu-ECP**, Eu-2,3-pyrazine dicarboxylic acid; **Cu@Eu-BTC**, Cu@Eu-Trimesic acid.

References

1 Pengfei Huang, Jiawei Lei, Zhirong Sun, Xiang Hu, *Chemosphere*, 2021, **268**, 129157.

2 N. Wang, M. Xie, M. Wang, Z. Li and X. Su, *Talanta*, 2020, **220**, 121352.

3 Q. Du, P. Wu, P. Dramou, R. Chen and H. He, *New J. Chem.*, 2019, **43**, 1291–1298.

4 S. Dadkhah, A. Mehdinia, A. Jabbari and A. Manbohi, *Microchim. Acta*, 2020, 187(10): 1-12..

5 X. Ling, R. Shi, J. Zhang, D. Liu, M. Weng, C. Zhang, M. Lu, X. Xie, L. Huang and W. Huang, *ACS Sensors*, 2018, **3**, 1683–1689.

6 F. Moghzi, J. Soleimannejad, E. C. Sañudo and J. Janczak, *ACS Appl. Mater. Interfaces*, 2020, **12**, 44499–44507.

7 J. Wang, R. Du, W. Liu, L. Yao, F. Ding, P. Zou, Y. Wang, X. Wang, Q. Zhao and H. Rao, *Sensors Actuators, B Chem.*, 2019, **290**, 125–132.

8 K. Chaiendoo, S. Ittisanronnachai, V. Promarak and W. Ngeontae, *Carbon N. Y.*, 2019, **146**, 728–735.